

VERTICAL LAND MOTION AND INUNDATION PROCESSES BASED ON THE INTEGRATION OF REMOTELY SENSED DATA AND IPCC AR5 SCENARIOS IN COASTAL SEMARANG, INDONESIA

Muhammad Rizki Nandika^{1*,2}, Setyo Budi Susilo¹, Vincentius Siregar¹

¹ Marine Technology Department, IPB University, 16680 Bogor, Indonesia

² Indonesian National Institute of Aeronautics and Space, 13220 Jakarta, Indonesia

*e-mail: rizki.nandika@gmail.com

Received: 10 December 2019; Revised: 14 February 2020; Approved: 14 February 2020

Abstract. Vertical land motion (VLM) is an important indicator in obtaining information about relative sea-level rise (SLR) in the coastal environment, but this remains an area of study poorly investigated in Indonesia. The purpose of this study is to investigate the significance of the influence of VLM and SLR on inundation. We address this issue for Semarang, Central Java, by estimating VLM using the small baseline subset time series interferometry SAR method for 24 Sentinel-1 satellite data for the period March 2017 to May 2019. The interferometric synthetic aperture radar (InSAR) method was used to reveal the phase difference between two SAR images with two repetitions of satellite track at different times. The results of this study indicate that the average land subsidence that occurred in Semarang between March 2017 and May 2019 was from (-121) mm/year to + 24 mm/year. Through a combination of VLM and SLR scenario data obtained from the Intergovernmental Panel on Climate Change (IPCC), it was found that the Semarang coastal zone will continue to shrink due to inundation (forecast at 7% in 2065 and 10% in 2100).

Keywords: *relative sea-level rise, interferometry, remote sensing, InSAR*

1 INTRODUCTION

As a country composed of many small islands and extensive coastal areas, Indonesia has a high level of vulnerability to sea-level rise (SLR) events. SLR itself not only causes inundation events, but also presents more serious dangers. If the projected rise in sea level due to global warming occurs, then the vulnerability to tropical cyclone storm surge flooding will increase (Dasgupta, Laplante, Murray, & Wheeler, 2009; Brecht, Dasgupta, Laplante, Murray, & Wheeler, 2012). Rising sea levels will also contribute to the erosion of sandy beaches and low-altitude islands (Sherman & Bird, 1995). Thus, a good understanding of sea-level changes will be very helpful in correcting uncertain information related to SLR predictions.

Previous studies have identified that SLR caused by climate change is not the only parameter that affects the inundation of an area. Vertical land motion (VLM) is also an important phenomenon in generating inundation risk (Douglas, 1991, 2001; Blewitt et al., 2010; Hanson, et al., 2011; Martínez-Asensio et al., 2019). In some cases, VLM can have a greater influence than SLR caused by climate change (Wöppelmann & Marcos, 2016; Pfeffer, Spada, Mémin, & Boy, 2017). Isostatic changes resulting from the melting of ice and glacial isostatic adjustments are also known to cause changes in sea level across the entire surface of the Earth (Peltier, Farrell, & Clark, 1978; Massey et al., 2008; Sweet et al., 2017). It is therefore very important to consider these parameters in evaluating how

changes in sea level may affect coastal areas and small islands.

Although it has been recognized that VLM plays a key role in developing understanding of future sea levels, information about it is difficult to obtain. Conventional observations using the Global Positioning System (GPS) and the levelling method can be done, but with limited time, money and human resources, observations on a large scale will be difficult to carry out. To overcome this limitation, remote-sensing technology using the interferometric synthetic aperture radar (InSAR) method has been widely used for wide-range deformation and long-term temporal observation (Le Cozannet et al. 2015; Anjasmara, Yusufiana, Kurniawan, Resmi, & Kurniawan, 2017; Cian, Blasco, & Carrera, 2019; Poitevin et al., 2019; Vadivel et al., 2019).

The expected result of this study is the prediction of inundation through several scenarios of SLR. We addressed this issue for Semarang, Central Java, because of its densely populated coastal area. The results obtained from this study can also be used as important information in managing areas sustainably.

2 MATERIALS AND METHODOLOGY

2.1 Location and data

Semarang City (Figure 2-1) is located on the north coast of Java Island between 6°50'–7°10' and 109°35'–110°50'. The area is bordered by Kendal Regency to the west, Demak Regency to the east, Semarang Regency to the south and the Java Sea to the north. The coastline is 13.6 km in length and has land height of between 0.75 and 348 meters above sea level.

Based on population projections calculated in 2018, 1,786,114 people are living in Semarang City, with an average annual growth rate in 2015–2016 of 1.64%. The density of population of the Semarang region in the past five years has caused land subsidence to occur in this region.

Geologically, Semarang is formed from several types of deposits, including breccia rocks, volcanic breccia rocks, volcanic rocks, marine layers, volcanic deposits and alluvial deposits. In coastal areas, the soil type is dominated by alluvial deposits. The characteristics of alluvial deposits are that they are still experiencing consolidation and compaction. This process can lead to subsidence events (Sophian, 2010).

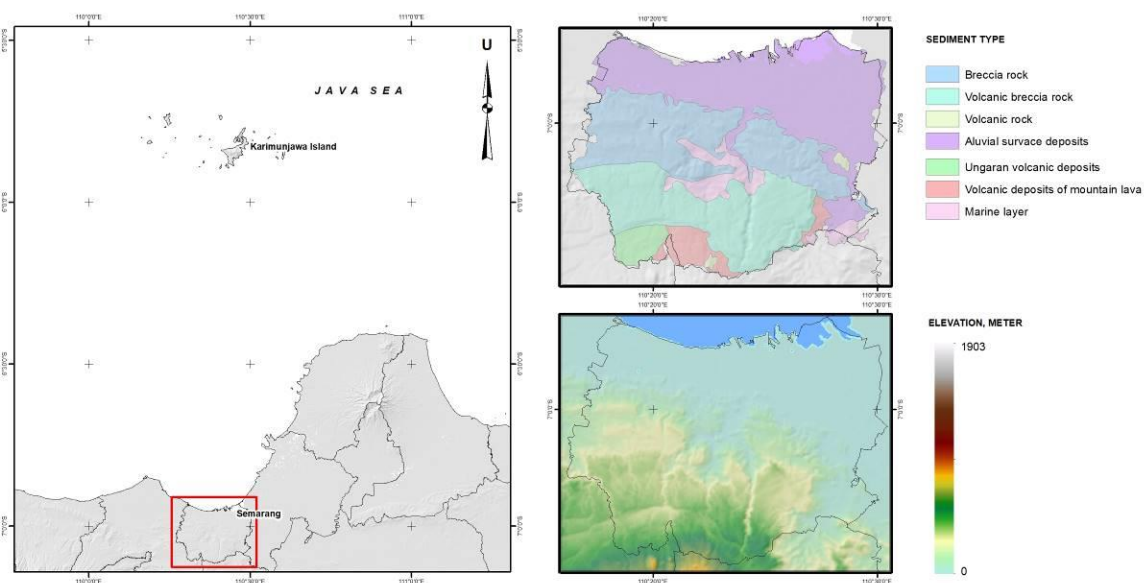


Figure 2-1: Semarang: environmental conditions

The spatial data used consist of 24 interferometric wide mode (IW) Sentinel 1A single look complex (SLC) satellite images acquired from March 2017 to May 2019. We also used the digital elevation model (DEM) owned by the Geospatial Information Agency (DEMNAS) published in 2018 as the current DEM reference data. The tabular data used are four scenarios of SLR from the IPCC: representative concentration pathway [RCP] 2.6 2065; RCP 2.6 2100; RCP 8.5 2065; and RCP 8.5 2100.

2.2 Vertical land motion assessment

SAR images produce two important items of information in each pixel: amplitude (backscatter) and phase (range). Amplitude is related to the energy of the backscattering signal recorded by the sensor, while phase is related to the distance of the sensor from the target (Ismullah, 2004; Zhou Chang, & Li, 2009). As ground height changes, the distance between the sensor and the ground changes, and this affects the magnitude of the phase recorded by the SAR sensor.

SAR interferometry is used to calculate interference patterns caused by phase differences between two SAR images, where this information is processed from satellite repetitions at two different times (Massonnet & Feigl, 1998). The phase difference value ($\Delta\phi$) of this pair of images contains five contributions, consisting of phase contributions reflecting orbit position ($\Delta\phi_{orb}$), topography ($\Delta\phi_{top}$), atmosphere ($\Delta\phi_{atm}$), surface deformation ($\Delta\phi_{def}$) and noise ($\Delta\phi_{noise}$) (Equation 1).

$$\Delta\phi = \Delta\phi_{orb} + \Delta\phi_{top} + \Delta\phi_{atm} + \Delta\phi_{def} + \Delta\phi_{noise} \quad (2-1)$$

To obtain the value of deformation, all contributions other than the deformation phase value ($\Delta\phi_{def}$) must

be omitted.

While the interferometry method can be used to see phase difference due to surface deformation, a large amount of SAR data can be used to see the rate of deformation. Using extensive SAR data can reduce the decorrelation that occurs during the interferogram process, so that the average value of the line-of-sight (LoS) velocity is obtained more accurately (Ferretti, Prati, & Rocca, 2001). The method used in processing ground vertical-motion data is the time series InSAR (TS-InSAR) method together with the small baseline subset (SBAS) technique. SBAS was chosen because it is an effective technique in overcoming temporal and perpendicular differences in the radar data.

There are 11 steps that must be carried out to process ground-surface movement data using the SBAS technique: 1) DEM conversion; 2) coregistration; 3) selection of image pairs; 4) DInSAR processing; 5) pixel filtering; 6) flat-earth phase removal; 7) topography effect removal; 8) coherence threshold; 9) unwrapping; 10) SBAS algorithm; and 11) geocoding.

2.3 Sea-level scenarios

Future changes in ocean volumes caused by global warming have been explained in a report published by the IPCC (AR5). The SLR projections provided are for 2065 and 2100, illustrating global SLR for the mid and late 21st century. These scenarios are formed through various combinations of climate scenarios and are designated as representative concentration pathways (RCPs). In this study, the sea-level scenarios for RCP 2.6 and RCP 8.5, which are the best and worst climate scenarios, can be used to conduct hazard assessments. These values are reported in Table 2-1.

Table 2-1: Sea-level scenarios obtained from the IPCC.

Scenarios	Year	Projected sea level (m)
IPCC RCP 2.6	2065	0.24 (0.17 – 0.32)
	2100	0.44 (0.28 – 0.61)
IPCC RCP 8.5	2065	0.3 (0.22 – 0.38)
	2100	0.74 (0.52 – 0.98)

2.3 Potential coastal inundation assessment

InSAR, VLM is used to define the future topography of the area. Assuming that the movement trend remains constant over time, the vertical rate in each InSAR is projected to estimate land variations between 2017 and 2019 and to predict future coastal topography (FDEM) in 2065 and 2100.

The assessment of the zones potentially exposed to inundation was performed by combining the FDEM with the sea-level scenario provide by the IPCC (Figure 2-2).

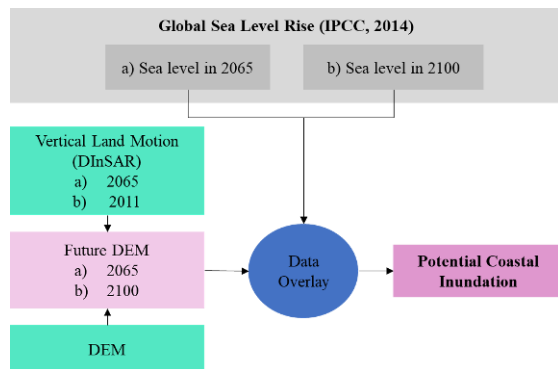


Figure 2-2: Steps for assessing coastal inundation hazards. Sea levels in 2065 and 2100 are estimated from the future rising rate provided by the IPCC. VLM was evaluated from satellite radar interferometry (InSAR) data analysis and projected to 2065 and 2100.

3 RESULTS AND DISCUSSION

3.1 Baseline plot

A good understanding of the selection of perpendicular/temporal baselines plays an important role in producing good quality interferograms. Large temporal differences in each pair

of images can result in temporal decorrelation due to changes in object conditions between observations. In addition, large perpendicular distance can cause spatial decorrelation that affects the geometry of the image.

To maximize the deformation processing using the small baseline technique, we set a threshold time of <90 days and a baseline threshold of <100 meters. Through this selection, we obtained 40 pairs of interferogram images which can be seen in Figure 3-1. The 40 data are then used to process displacement time series and mean LoS velocity.

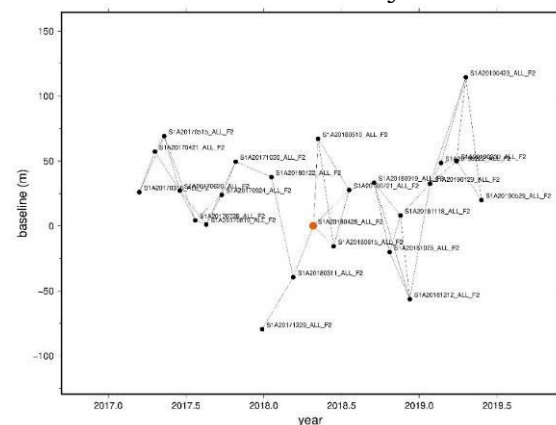


Figure 3-1: Baseline plot of 40 image pairs

3.1 Displacement time series

Displacement time series (disp1, disp2, disp3, ...) illustrate the change in time series for Semarang City in the period between 16 March 2017 and 29 May 2019. The time series displacement information is obtained by applying a least squares algorithm during the inversion process (Schmidt & Bürgmann, 2003).

Figure 3-2 shows the magnitude of the change in time series from March 2017 to May 2019. It can be seen that the north and northeast regions of Semarang City experienced significant subsidence, while the west and south parts of the city tended to be more stable.

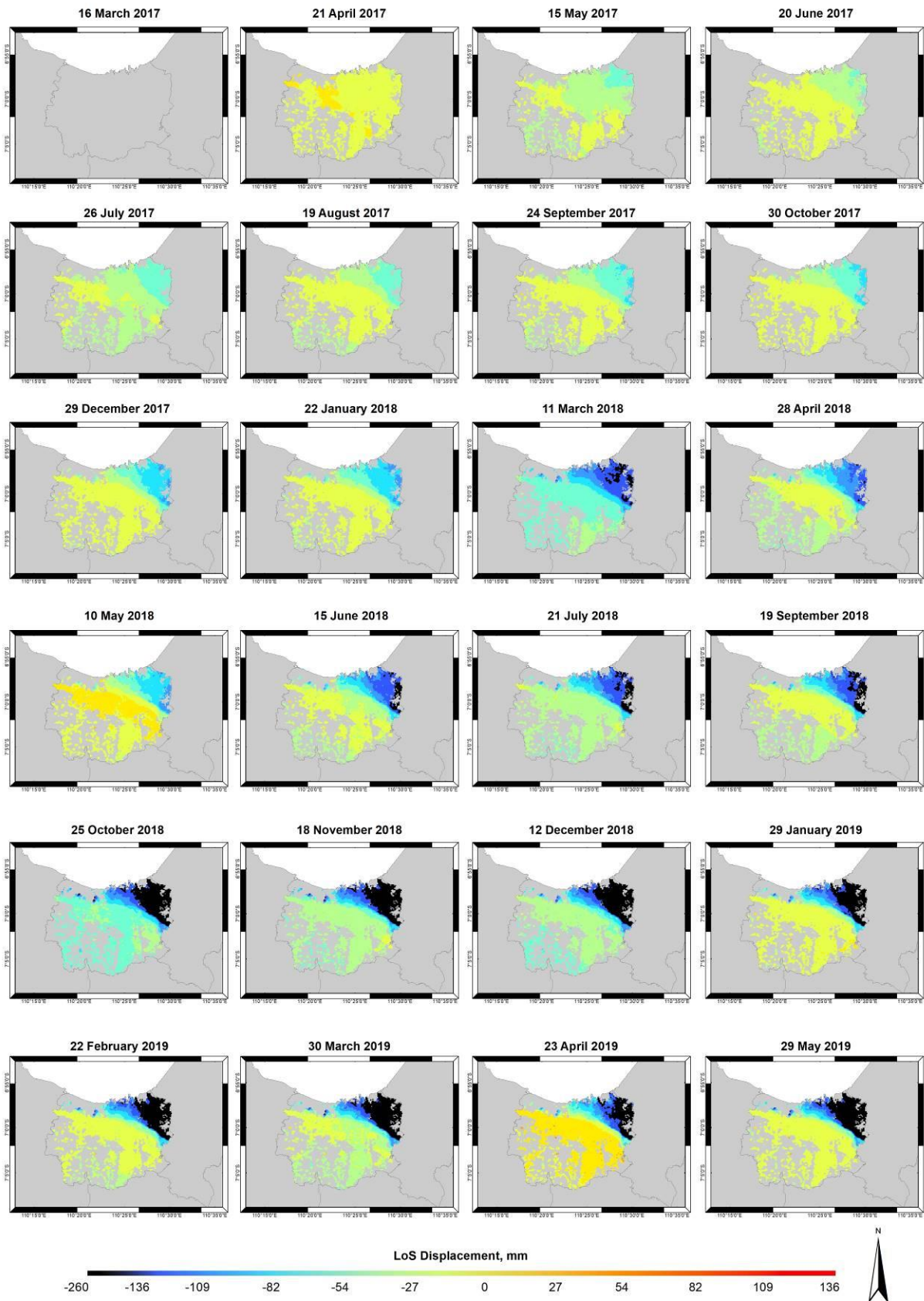


Figure 3-2: Displacement time series between 16 September 2017 and 29 May 2019. Red indicates uplift (+) while black indicates subsidence (-)

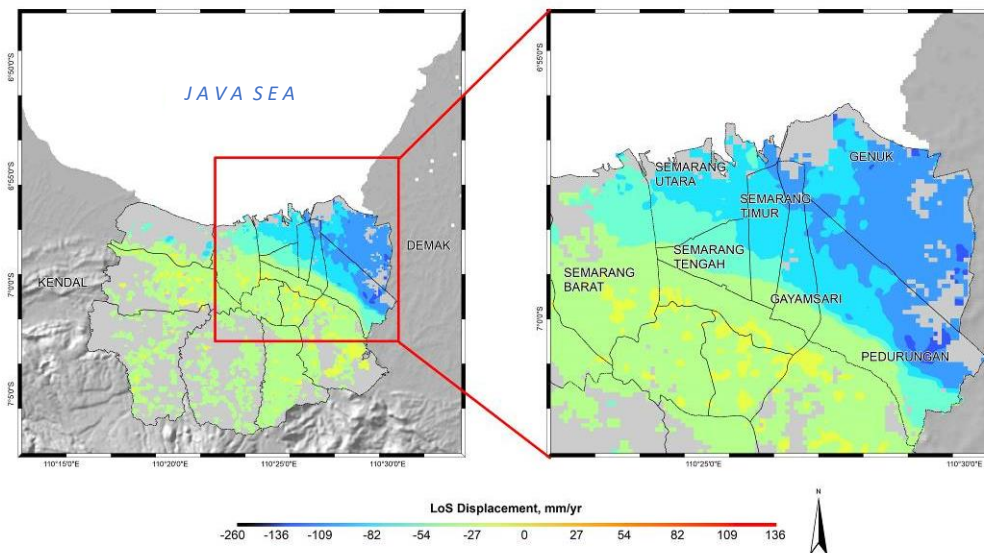


Figure 3-3: Mean LoS velocity for Semarang City from 15 March 2017 to 29 May 2019

3.3 Mean LoS velocity

Mean LoS velocity (vel_ll.grd) is information that shows the average deformation velocity of the 40 pairs of images between 16 March 2017 and 29 May 2019. Mean LoS velocity information was obtained by applying the least squares inversion and singular value decomposition (SVD) formula automatically, using the commands provided by GMTSAR.

Figure 3-3 explains the average deformation velocity that occurred in Semarang City from March 2017 to May 2019, of between -121 mm/year and +24 mm/year.

From the deformation patterns identified, it can be seen that the area to the north and northeast of Semarang City tended to decrease in height (subsidence). These areas include Genuk district, Pedurungan district, Gayamsari district, East Semarang District, Central Semarang district and North Semarang district.

The results obtained in this study are in line with similar recent studies that conducted in the city of Semarang

using DInSAR, in which Genuk district, Pedurungan district, Gayamsari district, East Semarang district, Central Semarang district and North Semarang district were found to be the areas with the highest subsidence rates (Islam, Prasetyo, & Sudarsono, 2017).

To calculate the average land subsidence by area, we divided the Semarang region into two areas based on the pattern of deformation that occurred (Figure 6). The results showed that land subsidence in the first area was -4.9 mm/year, while in the second area was -68.4 mm/year. This data could then be used to create a scenario of inundation.

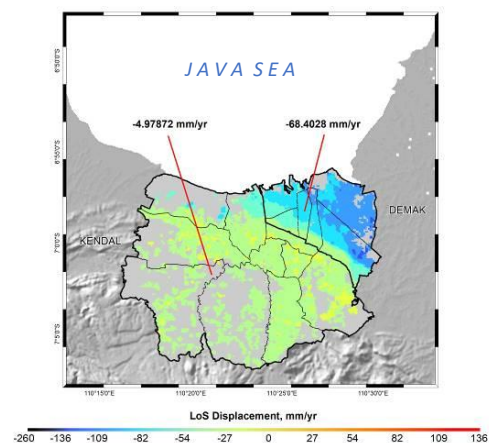


Figure 3-4: Mean LoS velocity by area

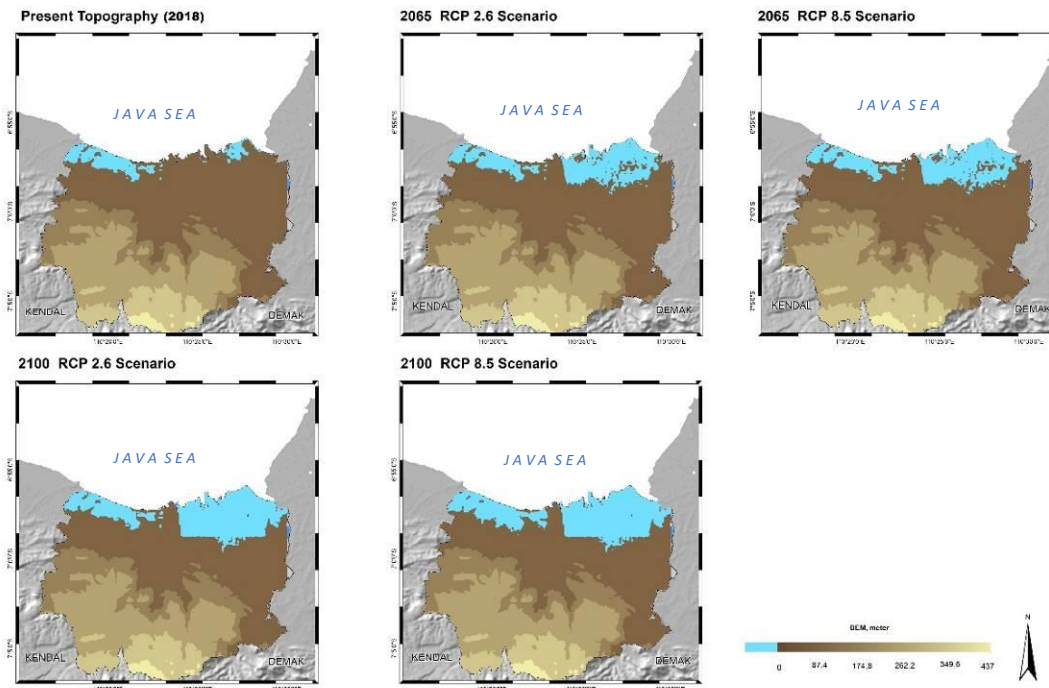


Figure 3-5: Comparison of present coastal topography, the 2065 scenario and the 2100 scenario derived from satellite radar interferometry (InSAR) and the IPCC scenarios

Table 3-1: Areas potentially exposed to the relative SLR effect in Semarang

Scenarios	Area (km ²)	Potentially inundated area (km ²)	Percentage
Present day	372.981532	-	-
2065 RCP 2.6	346.538192	26.44334	7.09%
2065 RCP 8.5	346.538192	26.44334	7.09%
2100 RCP 2.6	335.035932	37.9456	10.17%
2100 RCP 8.5	326.189864	46.791668	12.55%

3.4 Scenarios of inundation

By combining FDEM with sea-level scenarios provided by the IPCC, Semarang inundation models were obtained for several scenarios. Figure 7 shows the spatial inundation models for the four scenarios. Assuming that SLR and land subsidence continue to increase, flooding will continue to expand through to the scenario for 2100.

The Semarang region will continue to shrink due to widespread inundation. In the model for 2065, its area would decrease by 7%. In the 2100 model the shrinkage process has continued, reaching > 10% (Table 3-1).

4 CONCLUSIONS

Research on land subsidence integrated with the SLR scenarios for 2065 and 2100 has been successfully carried out to assess the inundation hazards that may occur in Semarang City.

Average land subsidence in Semarang between March 2017 and May 2019 was -121 mm/year to +24 mm/year. The northeast region of Semarang City experienced significant subsidence, including Genuk district, Pedurungan District, Gayamsari district, East Semarang district, Central Semarang district and North Semarang.

Through a combination of VLM and SLR scenario data obtained from the IPCC, it was calculated that the Semarang coastal zone would continue to shrink due to inundation, by 7% in 2065 and 10% in 2100.

Given that around 12.55% of the area will potentially be inundated by 2100 (RCP 8.5), proper management is needed to prepare for possible future sea-level-related impacts. However, further analysis could be done to improve the quality of the data, such as significant wave heights and currents that could cause erosion.

AUTHOR CONTRIBUTIONS

Vertical Land Motion and Inundation Process Based on the Integration of Remotely Sensed Data and IPCC AR5 Scenarios in Coastal Semarang, Indonesia. Lead Author: Muhammad Rizki Nandika; Co-Author: Setyo Budi Susilo and Vincentius Siregar.

REFERENCES

Anjasmara, I. M., Yusufania, M., Kurniawan, A., Resmi, A. L. C., & Kurniawan, R. (2017). Analysing surface deformation in Surabaya from Sentinel-1A data using DInSAR method. *AIP Conference Proceedings*, 1857. doi:10.1063/1.4987119

Blewitt, G., Altamimi, Z., Davis, J., Gross, R., Kup, C.-Y., & Lemoine, F. G. (2010). Geodetic observations and global reference frame contributions to understanding sea-level rise and variability. In J. A. Church, P.L. Woodworth, T. Aarup, & W. S. Wilson (Eds.), *Understanding sea-level rise and variability* (pp. 256–284). Hoboken, NY: Wiley-Blackwell.

Brecht, H., Dasgupta, S., Laplante, B., Murray, S., & Wheeler, D. (2012.) Sea-level rise and storm surges: High stakes for a small number of developing countries. *Journal of Environment & Development*, 21(1), 120–138.

doi:10.1177/1070496511433601

Cian, F., Blasco, J. M. D., & Carrera, L. (2019). Sentinel-1 for monitoring land subsidence of coastal cities in Africa using PSInSAR: A methodology based on the integration of SNAP and staMPS. *Geosciences*, 9(3), 124. doi: 0.3390/geosciences9030124

Dasgupta, S., Laplante, B., Murray, S., & Wheeler, D. (2009). Sea-level rise and storm surges: A Comparative Analysis of Impacts in Developing Countries. (Research Working Paper 4901) Washington, DC: World Bank Development Research Group.

Douglas, B. C. (1991). Global sea level rise. *Journal of Geophysical Research*, 96(C4), 6981–6992. doi:10.1029/91jc00064

Douglas, B. C. (2001). Chapter 3 sea level change in the era of the recording tide gauge. *International Geophysics*, 75, 37–64. doi:10.1016/S0074-6142(01)80006-1

Ferretti, A., Prati, C., & Rocca, F. (2001). Permanent scatterers in SAR interferometry. *IEEE Transactions on Geoscience and Remote Sensing*, 39(1), 8–20. doi:10.1109/36.898661

Hanson, S., Nicholls, R., Ranger, N., Hallegatte, S., Corfee-Morlot, J., Herweijer, C., & Chateau, J. (2011). A global ranking of port cities with high exposure to climate extremes. *Climatic Change*, 104, 89–111. doi:10.1007/s10584-010-9977-4

Islam, L. J. F., Prasetyo, Y., & Sudarsono, B. (2017). Analisis Penurunan Muka Tanah (Land Subsidence) Kota Semarang Menggunakan Citra Sentinel-1 Berdasarkan Metode DInSAR pada Perangkat Lunak SNAP [Semarang City land subsidence analysis using Sentinel-1 images based on the DInSAR method in SNAP software]. *J Geod Undip*, 6(2), 29-36

Ismullah, I. H. (2004). Pengolahan Fasa untuk Mendapatkan Model Tinggi Permukaan Dijital (DEM) pada Radar Apertur

- Sintetik Interferometri (INSAR) Data Satelit [Phase processing to obtain a digital surface height model (DEM) on synthetic interferometry aperture radar (INSAR) satellite data]. *ITB Journal of Science*.
doi:10.5614/itbj.sci.2004.36.1.2
- Le Cozannet, G., Raucoules, D., Wöppelmann, G., Garcin, M., Da Sylva, S., Meyssignac, B., ... Lavigne, F. (2015). Vertical ground motion and historical sea-level records in Dakar (Senegal). *Environmental Research Letters*, 10. <https://doi.org/10.1088/1748-9326/10/8/084016>
- Martinez-Asensio, A., Wöppelmann, G., Ballu, V., Becker, M., Testut, L., Magnan, A., & Duvat, V. (2019). Relative sea-level rise and the influence of vertical land motion at Tropical Pacific Islands. *Global and Planetary Change*, 176. doi:10.1016/j.gloplacha.2019.03.008
- Massey, A. C., Gehrels, W. R., Charman, D. J., Milne, G. A., Peltier, W. R., Lambeck, K., & Selby, K. A. (2008). Relative sea-level change and postglacial isostatic adjustment along the coast of south Devon, United Kingdom. *Journal of Quaternary Science*, 23, pp. 415–433. doi:10.1002/jqs.1149
- Massonnet, D. & Feigl, K. L. (1998). Radar interferometry and its application to changes in the earth's surface. *Reviews of Geophysics*, 36(4), 441–500. doi:10.1029/97RG03139
- Peltier, W. R., Farrell, W. E., & Clark, J. A. (1978). Glacial isostasy and relative sea level: A global finite element model. *Tectonophysics*. doi:10.1016/0040-1951(78)90129-4
- Pfeffer, J., Spada, G., Mémin, A., & Boy, J.-P. (2017). Decoding the origins of vertical land motions observed today at coasts. *Geophysics Journal International*, 210(1), 148–165. doi:10.1093/gji/ggx142
- Poitevin, C., Wöppelmann, G., Raucoules, D., Le Cozannet, G., Marcos, M., & Testut, L. (2019). Vertical land motion and relative sea level changes along the coastline of Brest (France) from combined space-borne geodetic methods. *Remote Sensing of Environment*. doi:10.1016/j.rse.2018.12.035
- Schmidt, D.A. & Bürgmann, R. (2003). Time-dependent land uplift and subsidence in the Santa Clara Valley, California, from a large interferometric synthetic aperture radar data set. *Journal of Geophysical Research Solid Earth*. doi:10.1029/2002jb002267
- Sherman, D. J. & Bird, E. C. F. (1995). Submerging coasts: The effects of a rising sea level on coastal environments. *Geographical Review*, 85(1), 111–113. doi:10.2307/215563
- Sophian, R. I. (2010). Penurunan Muka Tanah di Kota-Kota Besar Pesisir Pantai Utara Jawa (Studi Kasus: Kota Semarang) [Land subsidence in large coastal cities in the north coast of Java (Case Study: Semarang City)]. *Bulletin of Scientific Contribution* 8(1), 41–60
- Sweet, W. V., Kopp, R. E., Weaver, C. P., Obeysekera, W. J., Horton, R. M., Thieler, E. R., & Zervas, C. (2017). *Global and regional sea level rise scenarios for the United States*. NOAA Technical Report NOS CO-OPS 083. Washington, DC: NOAA/NOS Center for Operational Oceanographic Products and Services.
- Vadivel, S. K. P., Kim, D. J., Jung, J., Cho, Y.-K., Han, K.-J., & Jeong, K.-Y. (2019). Sinking tide gauge revealed by space-borne InSAR: Implications for sea level acceleration at Pohang, South Korea. *Remote Sensing*, 11(3), 277. doi:10.3390/rs11030277
- Wöppelmann, G. & Marcos, M. (2016). Vertical land motion as a key to understanding sea level change and variability. *Reviews of Geophysics*, 54, 64–92. doi:10.1002/2015RG000502
- Zhou, X., Chang, N.-B., & Li, S. (2009). Applications of SAR interferometry in

Muhammad Rizki Nandika et al.

earth and environmental science
research. *Sensors*, 9, 1879–1912.
doi:10.3390/s90301876

